Object-based Probabilistic Full Waveform Tomography

Paul Käufl[1], Andreas Fichtner[1], Heiner Igel[2]

kaeufl@geo.uu.nl

[1] Department of Earth Sciences, Utrecht University, The Netherlands, [2] Department of Earth and Environmental Sciences, Ludwig-Maximilians-Universität München, Munich, Germany

Universiteit Utrecht

1 Introduction

Recent developments in computational seismology allow for highly accurate modelling of wave propagation in strongly heterogeneous media. This enables us to use full seismograms as a data source for tomographic inversions. The classical approach to seismic tomography, however, consists of finding one single velocity model of the Earth's interior that minimises the misfit between simulated and observed seismograms. It does thus not account for the possible existence of multiple solutions that explain the data equally well, and it does not provide information on the reliability of a model.

We circumvent this issue by making use of a Monte Carlo optimisation method based on a Bayesian statistical framework. This leads to an ensemble of models and to an error estimate for each model parameter. We use the spectral-element method for the simulation of 3D wave propagation through heterogeneous Earth models. An object-based parametrisation of the Earth, motivated by the geological structure of western and central Australia, enables us to limit the dimensionality of the model space and to test hypothesis efficiently.

We apply our methodology to the Australian continental lithosphere. This is intended to answer the following questions: (1) How good is the resolution of the tomographic models? (2) Is there reliable information on density variations in the upper mantle contained in the waveforms? (3) How robust is the frequently inferred low-velocity layer around 150 km depth beneath Proterozoic Australia?

2 Geological structure

- Identification of **two large-scale ($\gtrsim 1500\ km$) structural elements** in continental Australia: the Archean cratons in the west and the predominantly Proterozoic units in the centre.
- Both Archean and Proterozoic lithosphere have been imaged consistently in several recent studies ([1, 10, 4, 5, 2, 3]). Significant differences between the tomographic images are limited to length scales below about 1500 km.
- Archean lithosphere is marked by anomalously high S wave speeds reaching $+8\,\%$ with respect to the radial average on a 1500 km length scale.
- Elastic properties of the Proterozoic lithosphere are strongly depth-dependent with a **structural boundary located at around 150 km depth**.

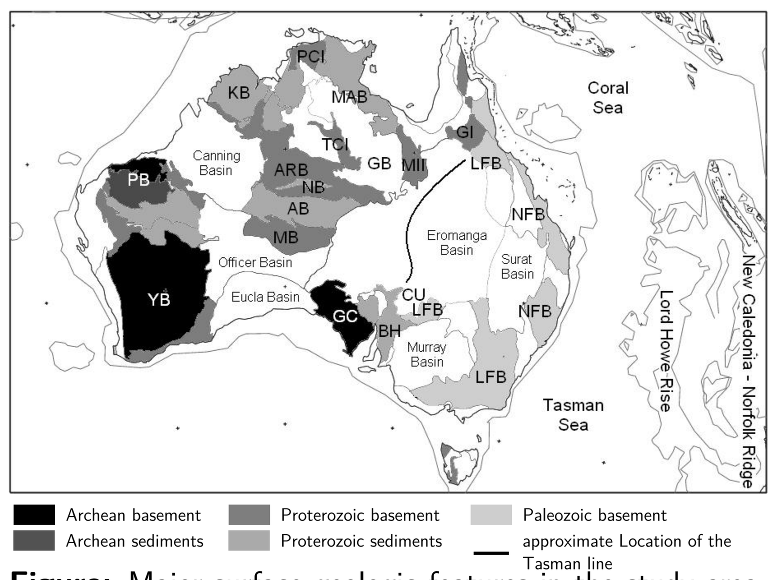

Figure: Major surface geologic features in the study area. Adapted from Myers et al. (1996).

AB - Amadeus Basin, ARB - Arunta Block, BH - Broken Hill Block, CU - Curnamona Block, GB - Georgina Basin, GC - Gawler Craton, GI - Georgetown Inlier, KB - Kimberley Block, LFB - Lachlan Fold Belt, MAB - McArthur Basin, MB - Musgrave Block, MII - Mount Isa Inlier, NB - Ngalia Basin, NFB - New England Fold Belt, NVP - Newer Volcanic Province, PB - Pilbara Block, PCI - Pine Creek Inlier, YB - Yilgarn Block

3 Object-based model construction

a) Definition of four basis functions b_i according to the geological structures in the study area in two layers from 0 to 150km and from 150km to 230km, respectively.

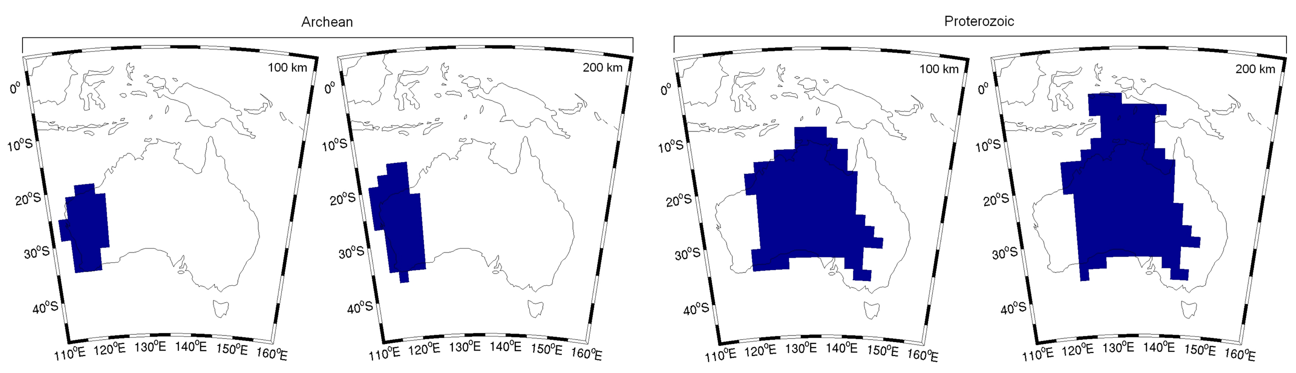

b) 3D Earth models $m(\mathbf{x})$ are constructed as filtered superpositions of weighted basis functions b_i, which take the value one within and zero outside the object. The objects are surrounded by a tomographic Australia model from Fichtner et al. (2009).

$$\tilde{m}(\mathbf{x}) = m_0(\mathbf{x}) + \sum_{i=1}^{N} m_i\, b_i(\mathbf{x}) \quad (1)$$

$$m(\mathbf{x}) = (F * \tilde{m})(\mathbf{x}) \quad (2)$$

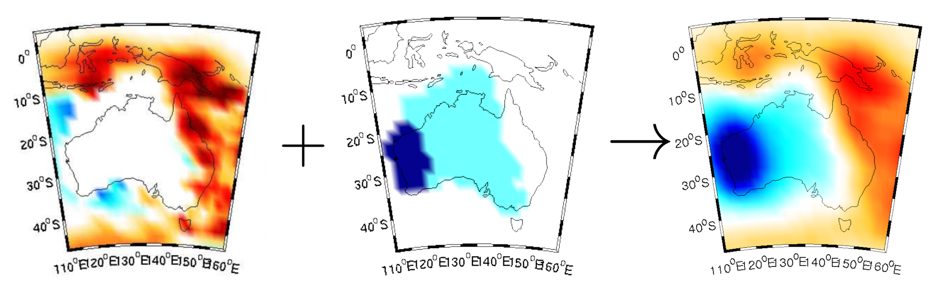

4 Data & Forward Modelling

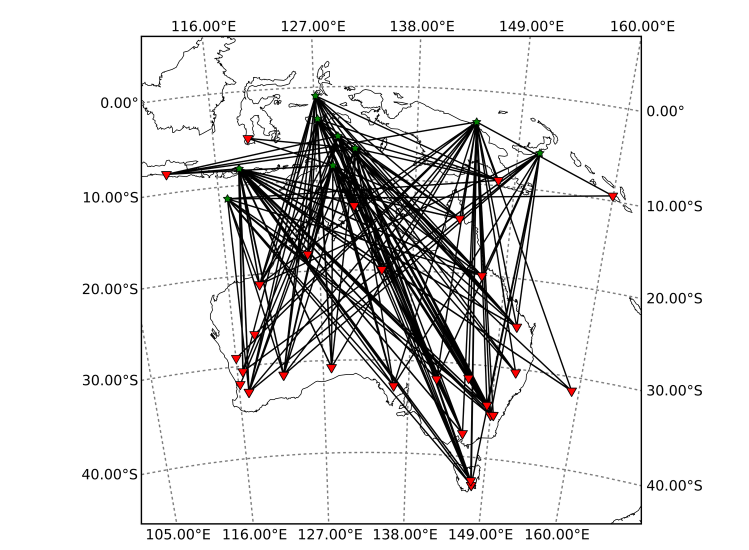

Observed data:

- primarily sensitive to the regions covered by the basis functions
- 338 vertical-component seismograms recorded at 30 different stations

Preprocessing:

- two frequency ranges from 60s to 200s and from 130s to 200s, in order to focus the sensitivity on the depth range of interest
- selection of the surface wave part by manually tapering each recording

Forward problem: We use a spectral element method as described by Fichtner et al. (2009) to simulate wave propagation in a spherical section ranging from $7.5°$ N to $50°$ S, from $105°$ E to $160°$ E and from the surface to 1461 km in depth.

- 25200 hexahedral elements with a size of approx. $1.6° \times 1.6° \times 73$km
- approximation of the wavefield by 4th order Lagrange polynomials collocated at the Gauss-Lobatto-Legendre points

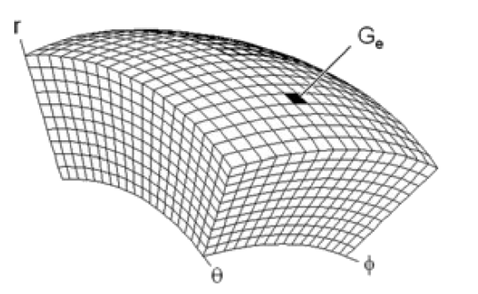

5 Probabilistic Inversion using the Neighbourhood Algorithm

Variation of P velocity- δv_p, S velocity- δv_s and density-perturbations $\delta\rho$ with respect to isotropic PREM in every object $\rightarrow$ **12-dimensional model space**.

The posterior probability density (PPD) of a model space vector $\mathbf{m}$ given a set of observed data $\mathbf{d}$ is given by

$$\sigma(\boldsymbol{m}|\mathbf{d}) = \frac{1}{\nu}\rho_M(\boldsymbol{m})L(\boldsymbol{m}|\mathbf{d}). \quad (3)$$

a) Choice of a uniform **prior probability density** $\rho_M(\boldsymbol{m})$ within the intervals:

$$\delta v_s \in [0; 0.6\,\text{km s}^{-1}] \quad (4)$$

$$\delta v_p \in [0; 0.8\,\text{km s}^{-1}] \quad (5)$$

$$\delta\rho \in [-0.4\,\text{g cm}^{-3}; 0.4\,\text{g cm}^{-3}] \quad (6)$$

b) Objective functional: A per-seismogram misfit is given by the L_1 distance between the L_1-normalised waveforms:

$$E(u_0, u) := ||u_0/||u_0||_1 - u/||u||_1||_1\,, \quad (7)$$

where $u_0(t)$ and $u(t)$ denote the observed and synthetic seismograms. A cumulative misfit $E(\mathbf{m})$ for model $\mathbf{m}$ is given by a weighted sum over the total number of recordings.

c) A natural choice for the **likelihood function** $L(\boldsymbol{m}|\mathbf{d})$ in terms of the cumulative misfit thus is:

$$L(\boldsymbol{m}) = \lambda^{N_d} \exp\left[-\lambda E(\mathbf{m})\right], \quad (8)$$

where the scale parameter $\lambda = 1/\sigma$ is related to the variance σ^2 of the observed seismograms, reflecting the noisy nature of the measurements.

d) Model space sampling: We use the Neighbourhood Algorithm (Sambridge, 1999) to sample the likelihood function quasi-randomly. The resulting ensemble of models gives an approximation of the joint PPD.

6 Results I - Posterior Probability Density

After 18 iterations the Neighbourhood Algorithm has generated 5000 models. From the approximate joint PPD marginal posterior distributions are retrieved by numerical integration. We observe three kinds of distributions:

- single-peaked, nearly Gaussian distributions (Archean and Proterozoic top layer S wave speeds)
- nearly exponential distributions (most densities and S wave speeds in the bottom layer) $\rightarrow$ might occur due to under-sampling or an insufficiently large parameter range, these parameters are thus excluded from interpretation
- nearly uniform distributions (most P wave speeds)

The results confirm

- high S wave speed perturbations (around $0.35\ km/s$) in the uppermost 150 km of Archean lithosphere. With 90% confidence values are higher than $0.1\ km/s$,
- slightly less pronounced S wave speed perturbations in the Proterozoic part, with values higher than $0.32\ km/s$ having a probability of less than 10%.

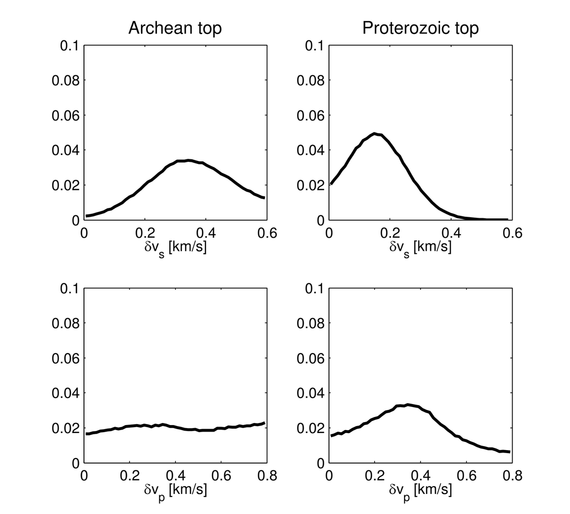

Figure: Marginal posterior distributions for top layer S and P wave speeds.

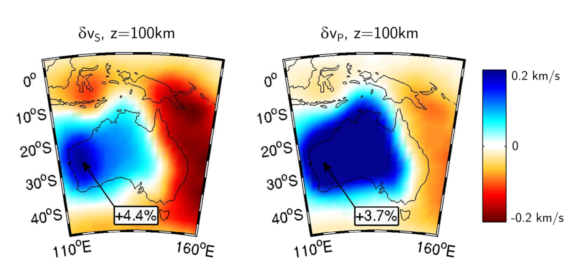

Figure: Horizontal slices through the most likely model in the ensemble.

7 Results II - Posterior Model Covariance

- Nearly uniform marginals for the P wave speeds indicate that each single parameter does not have a significant influence.
- The posterior covariance matrix, however, suggests a rather strong (anti-) correlation between the P wave speeds.

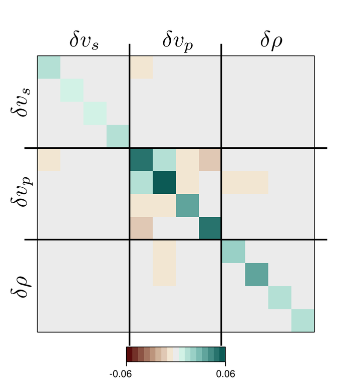

Posterior model covariance matrix. Row-order: Archean-top, -bottom, Proterozoic-top, -bottom.

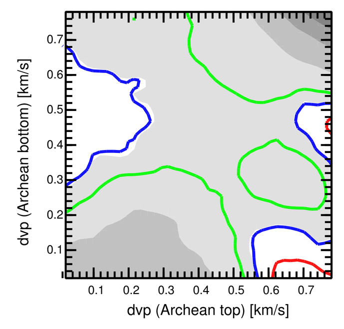

- The 2D marginal of Archean top layer vs. Archean bottom layer P wave speed (figure on the left) suggests that either both parameters take very high or very low values (green contour 60%, blue contour 90% and red contour 99% confidence)

8 Conclusion & Outlook

We showed that the methodology of a probabilistic full waveform inversion based on a regionalized parameterization works by inverting surface wave data to infer information about Australian continental lithosphere. Our results are consistent with recent tomographic studies. A future goal may be to relate the models endowed with error bars to results from mineralogical studies.

However, we note that we defer the interpretation of the density marginals, since we experienced problems possibly due to under-sampling. We note that these might be circumvented by using more informative prior distributions and a different initial tuning of the sampling algorithm.

9 References

[1] Debayle, E., Kennett, B. L. N., 2000. The Australian continental upper mantle: Structure and deformation inferred from surface waves, *J. Geophys. Res.*, **105**, 25423-25450.

[2] Fichtner, A., Kennett, B. L. N., Igel, H., Bunge, H.-P., 2009. Full seismic waveform tomography for upper-mantle structure in the Australasian region using adjoint methods, *Geophys. J. Int.*, **179**, 1703-1725.

[3] Fichtner, A., Kennett, B. L. N., Igel, H., Bunge, H.-P., 2010. Full Waveform Tomography for radially anisotropic structure: New insights into present and past states of the Australasian upper mantle, *Earth Planet. Sci. Lett.*, submitted.

[4] Fishwick, S., Kennett, B. L. N., Reading, A. M., 2005. Contrasts in lithospheric structure within the Australian craton - insights from surface wave tomography, *Earth Planet. Sci. Lett.*, **231**, 163-176.

[5] Fishwick, S., Reading, A. M., 2008. Anomalous lithosphere beneath the Proterozoic of western and central Australia: A record of continental collision and intraplate deformation?, *Precambrian Research*, **166**, 111-121.

[6] Myers, J. S., Shaw, R. D., and Tyler, I. M. (1996). Tectonic evolution of Proterozoic Australia. *Tectonics*, 15(6):1431–1446.

[7] Sambridge, M. (1999a). Geophysical inversion with a neighbourhood algorithm-i. searching a parameter space. *Geophysical Journal International*, 138(2):479.

[8] Sambridge, M. (1999b). Geophysical inversion with a neighbourhood algorithm–ii. appraisng the ensemble. *Geophysical Journal International*, 138(3):727.

[9] Tarantola, A. (2004). *Inverse Problem Theory and Methods for Model Parameter Estimation*. Society for Industrial and Applied Mathematics, Philadelphia, PA, USA.

[10] Yoshizawa, K., Kennett, B. L. N., 2004. Multimode surface wave tomography for the Australian region using a three-stage approach incorporating finite frequency effects, *J. Geophys. Res.*, **109**, doi: 10.1029/2002JB002254.